LEMRAP Laboratory

2021 Annual report

R. Bedogni (Resp.), C. Cantone

J.M. Gomez-Ros (Ass.), A. Pietropaolo (Ass.)

A. Lega (borsista), A. Calamida (Asseginsta), I.A. Castro Campoy (Ospite ICTP), A. Fontanilla (Ospite ICTP),

In collaboration with

INFN- LNF *Servizio Progettazione e Costruzioni Meccaniche*

Torino University and INFN section

ENEA Frascati

Summary

1. ENTER_BNCT experiment (2020 - 2022) - CSN 5

1.1 *Introduction*

Neutron Capture Therapy (NCT) is an alternative form of radiotherapy based on neutrons with energy in the keV - tens keV region (epithermal neutrons). The tumour cells are not directly killed by neutrons impinging the patient, but through a "sensitizer" agent in the form of a drug with the following main characteristics:

- Designed to ideally reach only malignant cells.
- Contains a high percentage of elements with high neutron interaction probability, or more precisely high neutron capture cross section
- This neutron absorbing material produces secondary ionising radiations as a result of the neutron capture, having the capability to kill the surrounding malignant cells. Neutron capture preferentially occurs in the thermal neutron domain.
- The secondary particles are preferably charged particles with energy in the order of MeV and range in the order of few to ten micrometers in tissue, so that the killing effect is limited to the labelled cell and the damage to surrounding healthy cells is limited.

Of the elements with highest thermal neutron capture cross-section, like 3-He, Cadmium, 10-Boron, 6-Lithium or Gadolinum, only Gadolinum and 10-Boron have been studied for NCT as they are practicably usable to mark pharmaceutical drugs. Gadolinium has higher cross section but the secondary particles, electrons and gammas, are weakly ionising if compared to the charged particles produced by neutron capture in 10-Boron. 10-B cross section is also very high (nearly 4000 barn) and produces highly ionising charged particles (alphas and tritons). Being 10-Boron the best candidate for NCT, this type of therapy is also called BNCT, Boron Neutron Capture Therapy.

It is worth mentioning how BNCT compares with radiotherapy with electrons/gammas and hadrons. Being definitively a charged-particle-based therapy, it is usually effective for tumours that resist to electrons and gammas. In this sense it is similar to hadron therapy. However, whilst hadron therapy is suited for tumours defined in space, BNCT operates a selection on a cell-by-cell basis. Thus it is suited for infiltrated tumours.

Current scientific challenges in BNCT are

- designing a drug that maximises the ratio between the Boron concentration in the tumour and that in the surrounding normal tissues (Boron uptake).
- maximising the thermal neutron fluence rate in the tumour location. As the human body is mainly water, it slows-down neutrons and tend to absorb them when they reach thermal energies. Thus a thermal neutron beam would be effective only for superficial tumours. By contrast, deep-seated tumours (up to about 6-8 cm) require epithermal neutrons: after being slowed-down in the surrounding tissues, they will reach the tumour with energy in the thermal domain. Neutron sources for BNCT are nuclear reactor or particle accelerators coupled with a neutron-producing target. Primary neutrons have MeV energies. A beam shaping assembly (BSA) is used to degrade the energy distribution of the primary neutrons to achieve the desired epithermal spectrum. BSAs are usually made of combinations of Teflon, Magnesium and Aluminum. The design of the therapeutic beam is done by very accurate Monte Carlo calculations. However, state-of-art techniques to experimentally verify the neutron spectrum are still limited, as they only measure energy-integrated quantities such as neutron activation in pure materials. Spectrometric techniques would be very desirable in BNCT, but are not currently implemented as neutron spectrometers are usually very complex and unsuited for routine scenarios. Also, very few neutron spectrometers simultaneously cover from thermal to MeV in energy. Bonner spheres fulfil this requirement, but they are cumbersome and do not work in real time. In addition, most existing neutron detectors do not operate in the very intense therapeutic fields encountered in BNCT.

1.2 *ENTER_BNCT project*

The ENTER_BNCT project aims to develop technical and measurement capabilities for the implementation of a centre for clinical BNCT (Boron Neutron Capture Therapy) based on a particle accelerator.

The project involves four INFN units: Pavia, Turin, LNL and LNF.

The main objectives of the project are:

- Developing a beryllium neutron target (LNL).

- Developing a Beam Shaping Assembly (made up of a new materials developed in previous project BEAT_PRO (Pavia).
- Design of the irradiation room and related tools (Pavia).
- Boron concentration measurements for clinical application (evaluations in the blood to determine irradiation time) and intra-cellular evaluation of boron distribution to calculate more precise dosimetry parameters (Pavia).
- Developing neutron measurements techniques for neutron beam quality assurance and patient dosimetry (LNF + Torino). The 2020 objective for LNF+Torino was the development of new neutron spectrometer able to work as routine tool for beam control in BCNT, called NCT-WES (Neutron Capture Therapy – Wide Energy Spectrometer)

1.3 *The NCT-WES neutron spectrometer*

NCT-WES (Neutron Capture Therapy – Wide Energy Spectrometer) is a new type of real-time neutron spectrometer able to work as routine tool for beam control in BCNT.
NCT-WES is a single-moderator-type spectrometer based on a collimated cylindrical structure, see Figure 1.1.

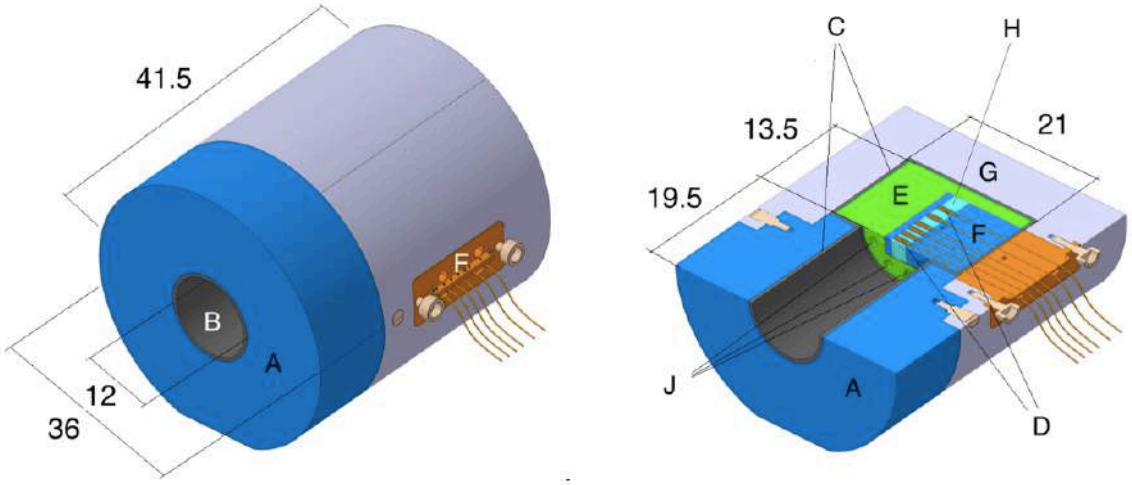

Figure 1.1: Schematics of the NCT-WES spectrometer. Quotes are in cm.

NCT-WES appears as a HDPE (high-density polyethylene) cylinder with diameter 36 cm and total length 41.5 cm. The dimensions of the cylinder as well as the location of detectors have been chosen to maximize the "spectrometric capability" of the device in the epithermal domain, i.e. the degree of differentiation between the response functions associated to different detector positions. The collimator (label A in Fig. 1) is 19.5 cm in length and its collimating aperture (label B), 12 cm in diameter, is internally lined with 0.5 cm of borated plastic SWX-238 from Shieldwerx (label C). Six thermal neutron detectors (D), located along the cylindrical axis, are contained in the HDPE capsule (label E, 20 cm in diameter, 13.5 cm in length). In order to facilitate maintenance, they are embedded in an extractable HDPE drawer (label F + label H). An external shield made of 0.5 cm of SWX-238 (label C) plus 7.5 cm of HDPE (label G) protects the capsule against neutrons arising from undesired directions. The centre of the shallowest detector is located at 0.72 cm depth from the end of the collimator. Detectors spacing (centre to centre) is 1.3 cm from the 1st to the 4th, and 2 cm from the 4th to the 6th. The detectors are parallelepipeds with external dimensions 0.32 cm x 1.5 cm x 1.3 cm and are connected through a 2 mm diameter coaxial cable. Their response is discussed in Section 3. It should be noted that NCT-WES can be adapted to allocate internal detectors with different size by simply replacing the polyethylene piece labelled H.

Label J refers to eight cylindrical air cavities, 1.3 cm in diameter, designed to enhance the response of deeper detectors relying on neutron streaming. The centres of these cavities are equally spaced on a circumference with radius 4.25 cm centred on the NCT-WES cylindrical axis.
The assembled NCT-WES is shown in Fig. 1.2.

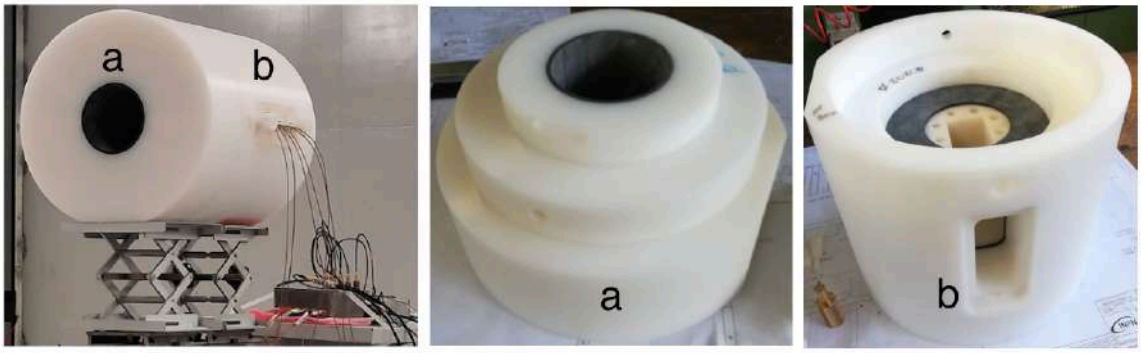

Figure 1.2. NCT-WES. On the left, the assembled prototype with the detector drawer inserted. At the centre, the part (a) including the collimator. On the right, the part (b) including the sensitive the capsule and its lateral protection. Air penetrations are visible. The drawer is extracted.

A Monte Carlo model was done to obtain the response matrix, obtaining the result in Figure 1.3.

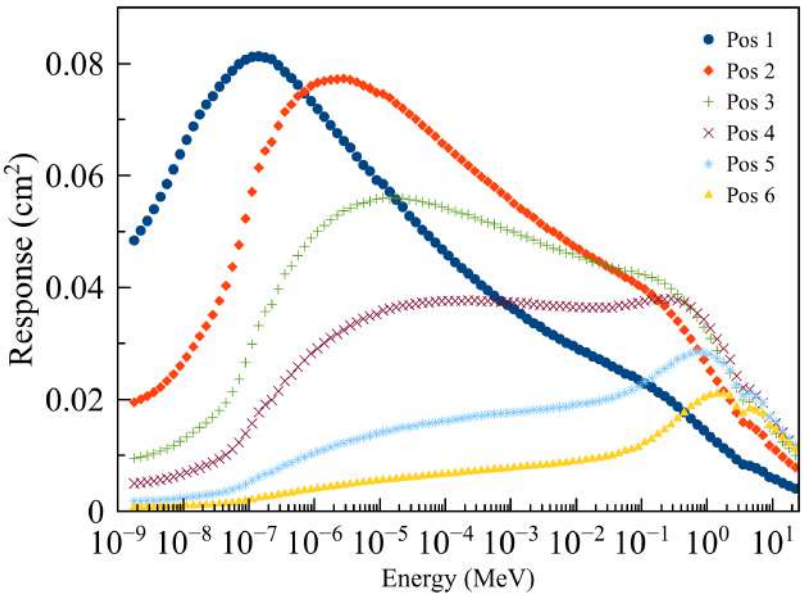

Figure 1.3. NCT-WES response matrix. The response is the expected number of measurable pulses in the TNPD, per unit incident fluence, as a function of the energy and the detector position.

1.4 *Silicon carbide detectors for the NCT-WES neutron spectrometer*

The NCT-WES spectrometer was built in 2020 and equipped with 1 cm^2 silicon thermal neutron detectors covered by 30 microns of ^6LiF. These detectors have sufficient sensitivity for calibration in typical low intensity reference neutron fields. In view of clinical applications with 1E+9 $cm^{-2}s^{-1}$ therapeutic epithermal beam these 1-cm2 detectors would be certainly prone to saturation and pile-up problems. Furthermore, the

high accumulated fluences would damage the Silicon in too short a time compared to a hypothetical routine use. Therefore, 1-mm^2 silicon carbide (SiC) detectors were studied, which are much smaller and resistant to radiation. V.
Silicon carbides are commercial Schottky diodes (SGLUX company) with 1.75 micron depleted region at bias voltage -12 V. They are coupled with a PVC disc on which a 30 micron layer of ^{6}LiF has been deposited. The detector records the secondary particles of the capture reaction

$$n + {}^6Li \rightarrow T + {}^4He$$

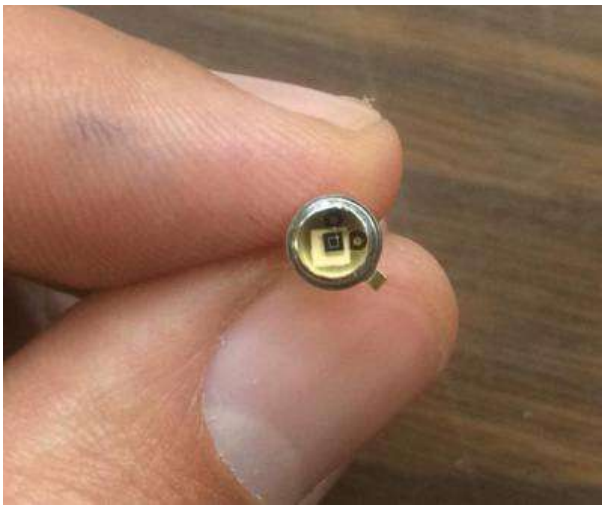

Fig. 1.4. SiC detector

After the application of the PVC screen deposited with 30 micron of ^{6}LiF, the SiC detectors were individually verified in the thermal neutron source called HOTNES (ENEA - INFN Frascati), which offers an isotropic field of thermal neutrons of 751 cm^{-2}s^{-1} ± 2% [1-3].

The measurement chain is composed of:

- Six-channels analog board, each consisting of CREMAT CR110 charge pre-amplifier and CREMAT CR200 shaper amplifier with 2 μs shaping time.
- +/- 12V stabilized low voltage generator
- Laboratory ADC / MCA system

The spectra recorded by the MCA (Fig. 1.5), show only a fraction (a few hundred keV) of the energy of the thermal capture products in ^{6}Li (alpha and Tritium) is released in the depleted region. Energies in the right tail refer to charged particles, which emitted at large angles by the converter, release larger energy. Secondary particles typically emitted in a direction orthogonal to SiC populate the peak around 200-300 mV. The amplitude-to-Energy conversion is approximately 1 MeV / V.

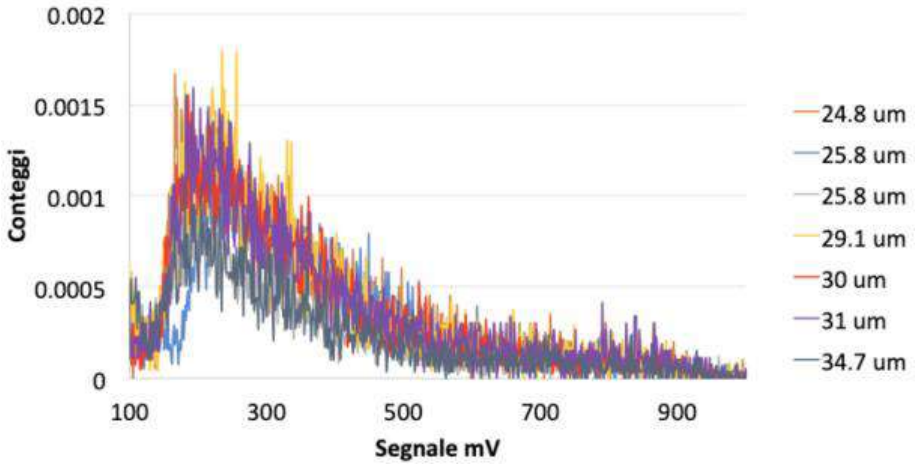

Fig. 1.5. Amplitude spectra of SiC acquired in HOTNES with the chain of Fig. 6.

Further testing campaign was performed using an ELECKTA LINAC Precise 18 MeV linear accelerator installed in the Physics Department of the University of Turin. Neutrons are produced via photonuclear reactions by directing the 18 MV high-energy photon beams from the linear accelerator into a 5-cm thick high-Z, Pb target. A large graphite block moderates the neutrons down to thermal energies [4,5].

The measurement system consists of the following:

- Six-channels analog board, each consisting of CREMAT CR110 charge pre-amplifier and CREMAT CR200 shaper amplifier with 2 μs shaping time.
- +/- 12V stabilized low voltage generator
- Laboratory ADC / MCA system

Figure 1.6 illustrates the count rate variation as a function of the dose rate. The dose rate linearity was measured from the 18 MV photon beam from the Elekta LINAC Precise. The SiC detector showed an excellent linear response with increasing dose rate (R^2=1) which also proves that the detector can withstand intense dose rate irradiation.

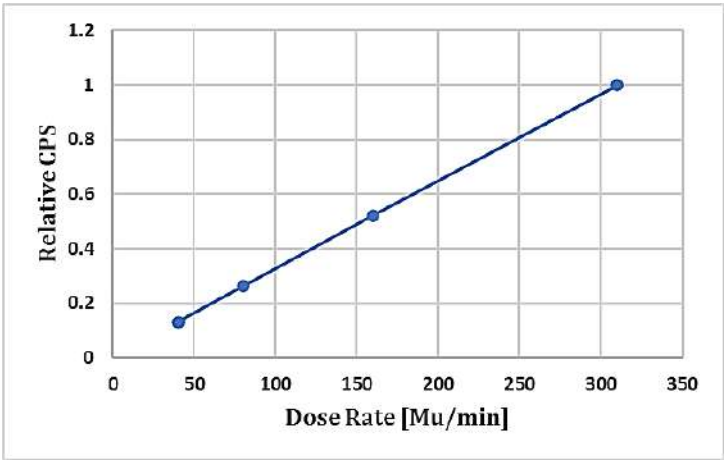

Figure 1.6. SiC detector response as a function of the incident photon dose rate

1.5 *NCT-WES calibration in a monoenergetic 3 MeV field*

The NCT-WES spectrometer was completed and firstly calibrated in 2020 at a reference Am-Be field at Politecnico di Milano [6]. NCT-WEs was presented in 2 online conferences:

27 Sept - 1 Oct. 2021 19th International Congress on Neutron Capture Therapy (19-ICNCT). Oral talk *R. Bedogni "Development of a single moderator neutron spectrometer for routine monitoring of therapeutic neutron beams"*

14-06-2021 to 18-06-2021. Herceg Novi (Montenegro). RAD2021 Conference. Oral communication V. Monti "*Single moderator active neutron spectrometer for therapeutic beam characterization in boron neutron capture therapy facilities*"

In 2021 a further calibration was performed at the 3 MeV monoenergetic beam produced at 0° from the D-D neutron target of the Frascati Neutron Generator (FNG), Fig. 1.7. NCT-WES operates as a "parallelized" Bonner Spheres Spectrometer, embedding six semiconductor-based thermal neutron detectors in a cylindrical moderator. Owing on a cylindrical collimating aperture, the device exhibits sharply directional response. To account for the non-uniform irradiation condition experienced in the near-target field, a dedicated NCT-WES response matrix was developed. The neutron spectrum, determined by means of the FRUIT unfolding code, is coherent with that previously derived with Bonner spheres.
FNG operated in D-D mode. An accelerated deuteron beam with energy between 245 and 260 keV impinged on a Titanium-coated copper target where deuterium atoms are implanted. The deuterium current ranged between 30 and 35 μA, leading to a source term between 3×10^{8} and 4×10^{8} s^{-1}. The expected monochromatic neutron energy in the forward direction was 3.1 MeV. The beam was monitored by means of a charged particle Silicon detector, placed at about 179° with respect to the primary beam and counting the ^{3}He particles from the ^{2}H(^{2}H,n)^{3}He fusion reactions.

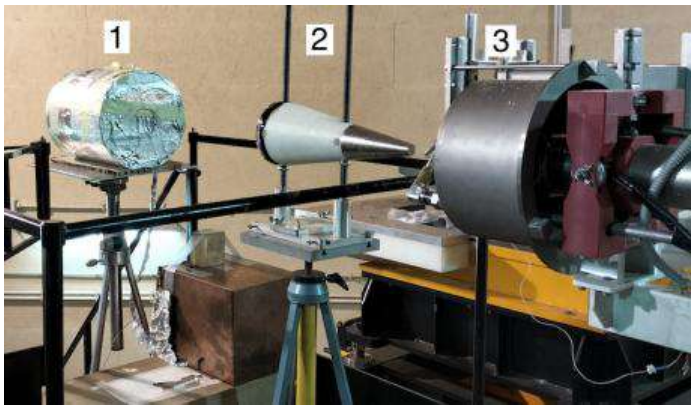

Figure 1.7 Picture of the setup for the near target field measurements at the FNG facility (see texyt for details).

The spectrometer was modelled using MCNP 6.2 including an accurate description of the TNPD internal detectors. The detector reading, intended as the number of pulses from alpha or tritium particles escaping the ^{6}LiF radiator and reaching the silicon active layer, was assumed to be proportional to the number of (n,t) capture reactions in the ^{6}LiF radiator. A point source located at 136 cm from the spectrometer front face was included in the simulation model, leading to determine the spectrometer response in terms of counts per emitted neutron as a function of the neutron energy and the detector position. The disadvantage of such approach is that the response matrix varies as the source-to-spectrometer distance varies.
The ENDF/B-VIII neutron cross section libraries below 20 MeV and room temperature cross section tables in polyethylene, S(α,β), were used. The scored quantity was the number of (n,t) events in the TNPD ^{6}LiF radiator. This was converted into a number of measurable pulses by applying a previously measured scaling factor F=(0.238±0.006) [6], defined as the number of measurable pulses per (n,t) capture reaction in the

^{6}LiF radiator of the TNPD. The response matrix is shown in Figure 1.8. The labels "Pos 1" to "Pos 6" in Fig. 3 indicate the detector positions, from the shallowest to the deepest one.
The maximum in the response functions shifts from fractions of eV (Pos 1) to few MeV (Pos 5 and Pos 6).

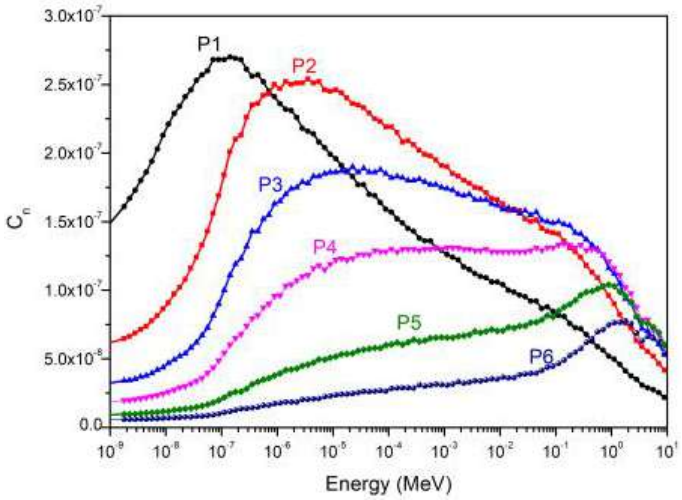

Figure 1.8: Figure 3. NCT-WES response matrix in terms of expected number of measured pulses in the TNPD, per emitted neutron, as a function of the energy and the detector position. Cn represents the counts per emitted neutron at 136 cm from the front-face (see text for details).
When plotting the un-collided normalised count against the detector position, the profile "Experimental" in Figure 1.9 is obtained. Uncertainties on this data (not shown in the figure for a better readability) are in the order of ±3% and arise from the quadratic combination of the counting statistics (±1%) and the detector-to-detector response variability (±3%).

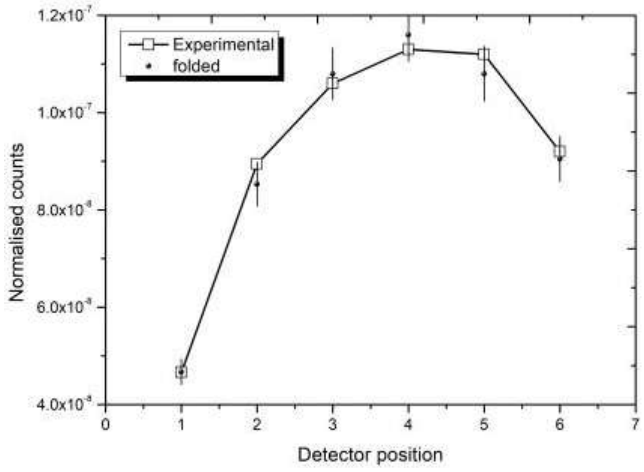

Figure 1.9: Experimental and "folded" normalised counts in the NCT-WES internal detectors exposed to the un-collided field (total field - shadow-cone). Only the uncertainties on the simulated profile (about 5%) are reported for a better readability. Line is only eye-guide.

Experimental data were unfolded using the FRUIT code [11]. As in the case of the Bonner spheres, the unfolding process is under-determined, as it pretends to determine a multi-group neutron spectrum starting from usually less than ten measurements (the normalised detector counts). Thus, the number of mathematical functions able at reproducing the experimental data, is potentially infinite. A way to orientate the unfolding code towards a physically acceptable solution is to complement the unfolding process with

some amount of pre-information, in addition to the response matrix, detector counts and related uncertainties. A "realistic" starting spectrum is the classical way to provide such pre-information. The unfolding code will fold the starting spectrum with the response matrix and "move" portions of neutron fluence from energy regions to others, attempting to reproduce the measured data. This iterative process has clearly limited energy resolution, so that fine structures such as narrow peaks will not appear in the resulting spectrum if they have not been introduced in the guess-spectrum. By contrast, the appearance of unexpected structures in the resulting spectrum often indicates that an inadequate starting spectrum was chosen.
To unfold the data from the current experiment, a previously determined Bonner spheres spectrum [12] was used as starting spectrum. Fig. 16 shows the starting spectrum as well as the unfolded one. Both fluence spectra are normalised to one count in the ^{3}He monitor and refer to a conventional distance of 100 cm, corresponding to the point where the Bonner Spheres were exposed in the comparison experiment of Ref. [12]. NCT-WES was exposed at a different distance (136 cm), and its spectrum was rescaled using the inverse square law to compare with BSS. It should be noted that whilst the BSS spectrum includes the component scattered by bulky metallic supporting structures, NCT-WES one only includes the un-collided one. So the first spectrum was expected to be larger than the second one, as evidenced by the results in Figure 1.10.

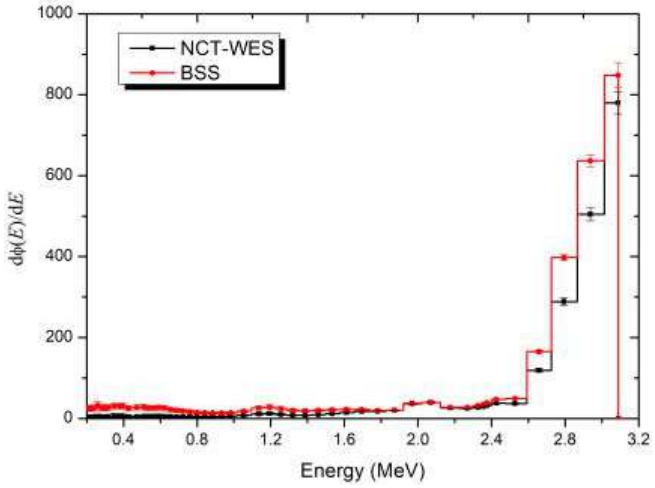

Figure 1.10: Starting (BSS) and unfolded (NCT-WES) spectra.

The reported spectra have uncertainties specified bin-by-bin. FRUIT derives these uncertainties by propagating uncertainties on the input quantities through the unfolding process [13].
A way to evaluate the unfolded spectrum is to apply it to the response matrix, deriving the so-called "folded counts", in turn comparing them to the "experimental counts". This is done in Fig. 15, showing a satisfactory agreement. Uncertainties of the folded counts are in the order of 5% and arise from the quadratic combination of:

- NCT-WES Monte Carlo modelling (±2%, based on [7])
- distance and alignment (±4%)
- unfolding process (±2.5%)

1.6 *CONES (compact neutron sensors)*

CONES detectors, to be used as spectrum-integrated clinical dosemeters in BCNT, should give an energy-integrated dosimetric indication on the three domains:

- thermal (E <0.4 eV),
- epithermal (0.4 eV <E <10 keV)
- fast (E> 10 keV)

and at the same time offer limited size to allow in typical water phantoms for BCNT, formed by tanks with a typical size of 30 cm.

For thermal neutrons, a SiC charged particle detector covered by 30 microns of 6LiF (see 2.1) has been hypothesized placed in the center of a small diameter high density polyethylene (HDPE) sphere. From the results of simulations performed with a diameter of 2 cm with the codes MCNP6 the response function of Figs 1.11 was obatined.

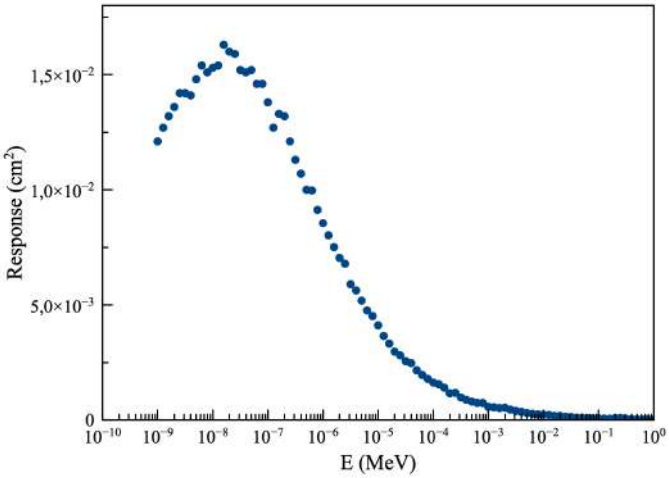

Fig. 1.11. MCNP response function of the 2 cm diameter configuration.

For epihtermal neutrons, a cylinder geometry was studied assuming height = diameter for a better isotropy. A preliminary simulation on the diameter showed that 70 mm guarantees a good compromise between flat energy response and small size.
It was decided to use high density polyethylene with a 1 mm thick internal cadmium insert to determine the shape of the response function.
The typical geometry is shown in Fig. 1.12 while the response function is shown Fig. 1.13.

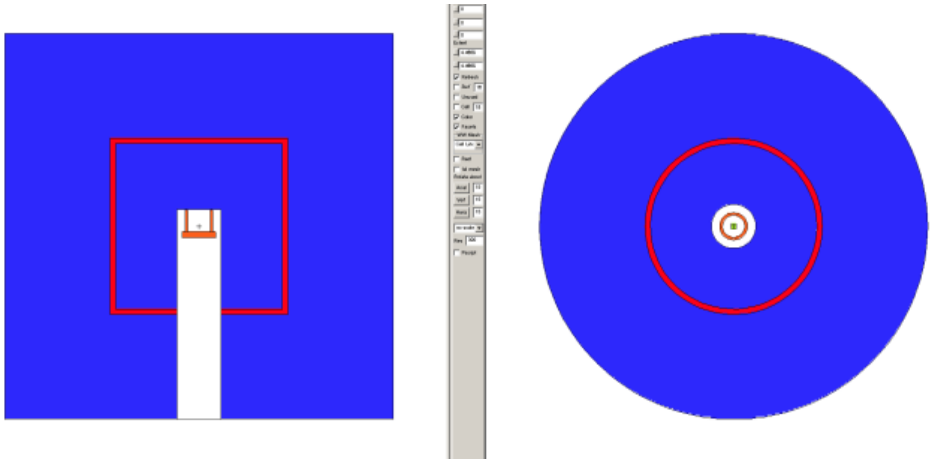

.

Fig. 1.12. CONES epithermal cylinder (height = diameter) in polyethylene with Cadmium insert. Internal diameter = 30 mm, external diam = 70 mm.

Fig. 1.1. Epithermal CONES. Cylinder geometry (height = diameter) in polyethylene with Cadmium insert. Response functions to varying internal cylinder diameter.

For fast neutrons, the same geometry as for epithermal CONES was maintained with a larger external diameter (10 cm). Dimensions are Internal diameter = 40 mm, external diam = 100 mm. See Fig. 1.13 for the response function.

The response functions of the thermal, epithermal and fast CONES probes are compared, each normalized to its maximum, in Fig. 1.13. It is evident how their combined use allows to obtain the desired energy-integrated responses in the thermal, epithermal and fast fields.

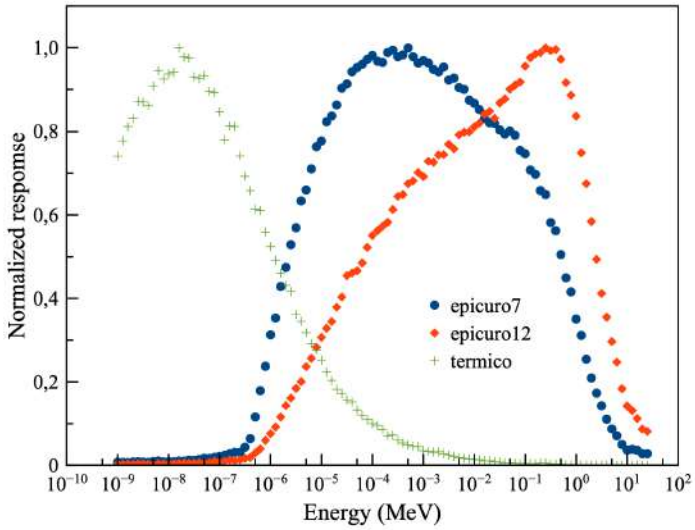

Fig. 1.13. CONES Response functions each normalized to its maximum.

CONES detectors were manufactured according to the simulation schemes called:
- thermal CONES: polyethylene sphere 2 cm in diameter (Fig. 20)
- epithermal CONES: Internal diameter = 30 mm, external diam = 70 mm.
- fast CONES: Internal diameter = 40 mm, external diam = 100 mm.

The built prototypes are presented in Figs. 1.14 - 1.16.

Fig. 1.14 - CONES built prototypes (1).

Fig. 1.15 - CONES built prototypes (2).

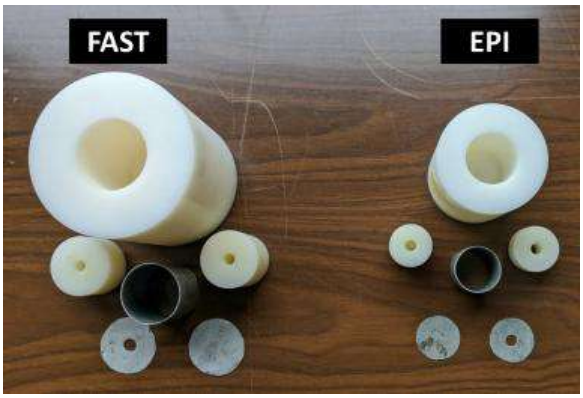

Fig. 1.16 - CONES built prototypes (2).

The following calibration fields were used for the CONES detectors (Table 1.1):

- **thermal field:** HOTNES thermal neutron facility at ENEA Frascati (Fig. 3) [1-3].

- **fast field:** the 3 MeV monoenergetic beam produced at 0° from the D-D neutron target of the Frascati Neutron Generator (FNG) (Section 2.2).

- **epithermal field**: LINAC-based epithermal field at Torino University developed within E_LIBANS project (20216-2018), where ah homogeneous epithermal field is achieved in a closed cavity (30 cm 30 cm x 20 cm), here briefly described.

Table 1.1. Calibration factor of CONES detectors.

Calibration Table (cm^{-2})	thermal field	epithermal field	3 MeV fast field
Thermal CONES	(3.42±0.05)E+3	(1.05±0.06)E+4	-
Epihtermal CONES	-	(1.00±0.05)E+4	(6.23±0.42)E+4
Fast CONES	-	(1.50±0.08)E+4	(1.91±0.11)E+4

2. SAMADHA (2021 - 2023) - CSN 5

2.1 *Introduction*

The SAMADHA project aims to investigate and study the neutron dose due to secondary neutrons produced by the interaction of cosmic particles with Oxygen and Nitrogen in atmosphere reaching the Earth below the South Atlantic Anomaly (SAA), a region in the planet with the lowest geomagnetic field where few or no data are available. This dose account for about one half of the effective dose received by humans at high-altitudes (ex. commercial flights 5000-7000 m). Ambient dosimetry campaigns will be performed in high altitude sites in the SAA area, to study the relation between dose rate and space weather/atmospheric phenomena particularly at the high-altitude Chacaltaya Lab (5240 m) Bolivia, and Mt. Famatina (5000 m) Argentina. Neutron spectrometry using a new spectrometer designed specifically for the measurement of cosmic neutrons will be done to provide an accurate neutron dose assessment and obtain information on the factors affecting the dose contributions such as environmental conditions.

The SAMADHA research group consists of multidisciplinary experts from dosimetry, cosmic ray physics, solar physics, space weather atmospheric physics, with experience in instrumentation and data analysis. INFN-LNF LEMRAP is one of the 5 collaborating groups and is responsible for:

- Design and construction of a Bonner sphere neutron spectrometer for measurements at high elevation.
- Ancillary systems for unattended operations.
- Monitor and data acquisition software.
- Data analysis and simulations.

The Bonner sphere spectrometer was completely built, characterised and calibrated in reference secondary standard field of 241Am-Be (Politecnico di Milano). See the details below:

- The following Bonner spheres have been built (diameters in mm): 80, 100, 120, 150, 170, 200, 200 with lead insert, 200 with iron insert. Complete Monte Carlo simulation was performed to derive the response matrix of the system. See 2.2.
- A set of 11 triaxially cabled 3He detectors (one per sphere + 3 spares) was prepared and a study was conducted to understand the relation between the signal amplitude and the cable length, see 2.3.
- The eight spheres will be acquired by two 6-channel analogue boards, see 2.4.
- The complete BSS system was calibrated in reference secondary standard field of 241Am-Be (Politecnico di Milano), allowing to validate the simulated response matrix with 2% overall uncertainty, see 2.5.

An extensive study was conducted to identify and minimise the sources of "spurious" pulses in the detectors, i.e. due to other causes than incident neutrons, such as electromagnetic interferences or spikes in the supply lines. If was found that

- compared to the conventional coaxial cabling of the 3He detectors, triaxial cabling of the 3He detectors prevents spurious pulses due to EM interferences. See 2.3.
- The high voltage generator (+ 850 V) is the major cause of spurious pulses. Specific studies were done. As a result, a massive capacitor-based filter on the high voltage ouptut was applied.
- The low voltage generator (dual +/-12 V) is the second cause of spurious pulses. Specific studies were done. As a result, a massive capacitor -based filter on the low voltage output was applied.
- The stability of the 220 Vac line is the third cause of of spurious pulses. This was reduced by applying an UPS.

The BSS is fully equipped, calibrated and operational. Field test at Plateau Rosa planned for July 2022. Shipment to South America can be expected to Autumn 2022.

2.1 *The SAMADHA spectrometer*

Diameters:

- 80 mm.
- 100 mm.
- 120 mm.
- 150 mm.
- 170 mm.
- 200 mm.
- 200 with lead-bullets insert (apparent density of bullets = 6.758 g/cm^3).
- 200 with iron-bullets insert (apparent density of bullets = 4.8094 g/cm^3).

The internal metal parts in lead or iron (steel) are needed to increase the response above 10 MeV. A "fluid" filling made of metal bullets is cheaper than solid inserts, and can be purchased at low cost near the final destination of the spectrometer, thus reducing the shipping costs.

Figure 2.1. Bonner spheres of the SAMADHA spectrometer.

After manufacturing, the spheres where mechanically characterised in terms of actual sizes and density of all parts, and a very realistic monte carlo modelling of their response was performed, see Figs. 2.1. and 2.2.

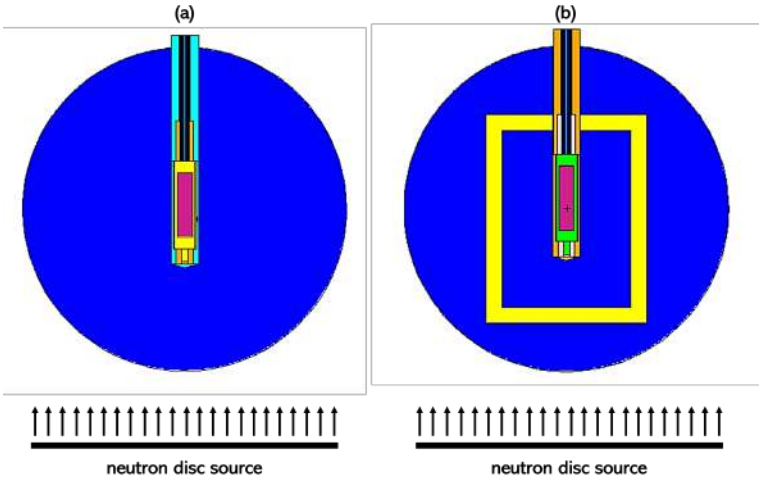

Fig. 2.2. Monte Carlo models used to simulate the response matrix of: (a) Spheres 80, 100, 120, 150, 170 and 200; and (b) Sphere 200 with Fe balls, and Sphere 200 with Pb balls.

The response functions for the SAMADHA spheres were simulated using the MCNP6 code for an extended neutron incidence energy range (from 1 meV to 5 GeV) to cover thermal to cosmic neutron energies. 130 logarithmic equidistant discrete energy bins were chosen for each detector-

sphere assembly. Figure 2.2 shows the detailed model of the SAMADHA spectrometer based on the actual dimensions and composition of each sphere and the specifications of the He-3 detector provided by the manufacturer. For spheres with Pb- and Fe-balls inserts, their density is taken to be ~60% of the theoretical densities of solid Pb and Fe, respectively, to account for the air gaps that were not filled in when using the metal balls. The source, modelled as a disc with the same dimension as the spheres being irradiated, emits parallel neutron beams to the sphere. Simulations were performed using the Bertini cascade and Dresner evaporation models with the RAL fission model. The ENDF/B VIII.0 nuclear data libraries and its corresponding thermal neutron scattering $S(\alpha, \beta)$ data were also employed in all the calculations. The h-poly.80t used in the code accounted for thermal neutron scattering by hydrogen bound in polyethylene. The F4 tally was used in the simulations to derive the neutron fluence as a function of energy within the active volume of the He-3 detector. The response is expressed in terms of the number of (n,p) reactions for He-3 per unit fluence as a function of energy. The response matrix for all the sphere-detector configuration of the SAMADHA spectrometer is shown in Figure 2.3. From the response functions, the system can completely characterize the energy distribution of the neutrons in a very large energy range. It can be observed that the maximum response, presented by the peak of the response functions, shifts from lower to higher energies with increasing sphere diameter. Large shift to higher energies for the large spheres is attributed to neutron thermalization in the sphere. Lower response function at the high energies is also evident due to elastic scattering with hydrogen in polyethylene. Spheres with the high-Z material inserts were also efficient in measuring neutrons above 20 MeV

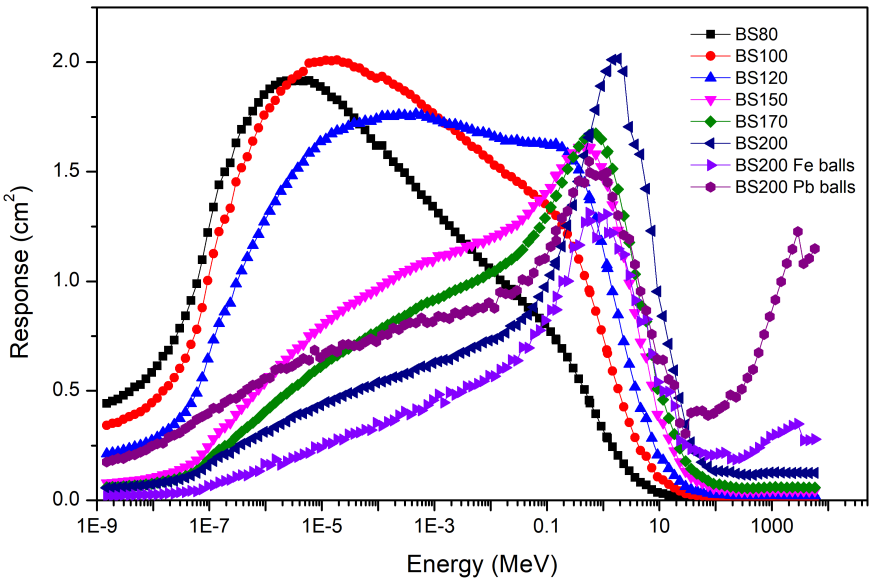

Figure 2.3. SAMADHA spheres response matrix calculated using the MCNP code.

2.3 *^{3}He detectors*

Compared to the conventional coaxial cabling, triaxial cabling of the ^{3}He detectors prevents spurious pulses due to EM interferences. All detectors were triaxially cabled. The detectors are He-3 VacuTec type 70 060. A total of eleven detectors were wired.

The response of the eleven He-3 neutron detectors upon exposure to thermal neutron field was tested in the ENEA HOTNES facility [1-3]. They were exposed to an isotropic field of thermal neutrons 751 $cm^{-2}s^{-1}$ (s.d. 2%).
The position of the full-energy peak (764 keV), corresponding to the collection of both secondary proton and triton from the neutron capture reaction in ^{3}He, depends on the length of the triaxial cable, see Table 2.1, Figs. 2.4 and 2.5.

Table 2.1. Corresponding Count Rate and Voltage Peaks of the He-3 detectors upon irradiation.

Detector	length (cm)	Vpeak (V)
ANET	102	0.683
120	120	0.651
80	130	0.666
100	128	0.653
150	147	0.657
170	150	0.625
200	160.4	0.642
new5	176	0.656
new3	178.5	0.628
new1	186.5	0.613
new4	191.5	0.650

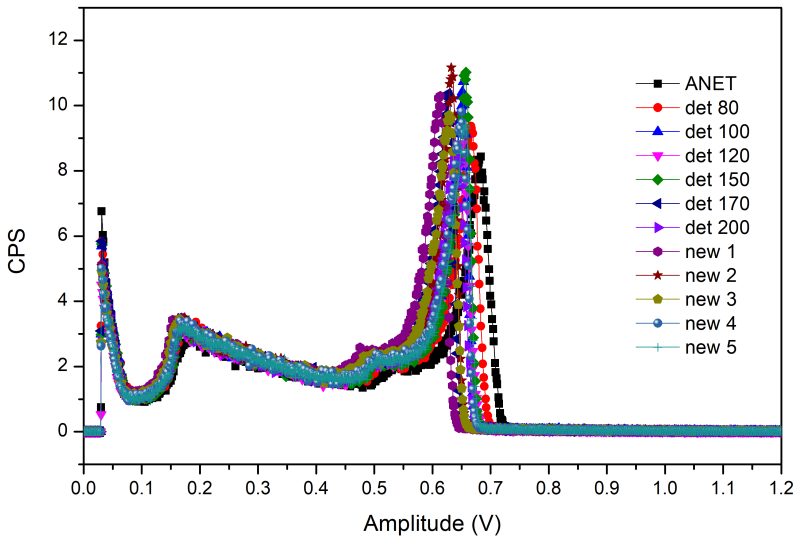

Figure 2.4. Spectra of the He-3 detectors exposed to thermal neutrons.

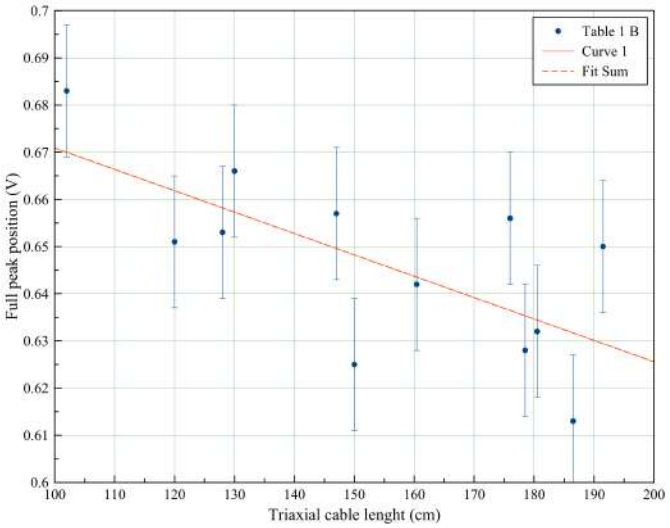

Figure 2.5**.** Relation between the triaxial cable length and the peak position.

2.4 *6-channel analogue boards*

The eight spheres will be acquired by two 6-channel analogue boards, so that 4 spare channels out of 12 will be available.
Every 6-channel analogue board include 6 analogue channels (one per detector). For every channel the circuit is composed by a charge preamplifier CREMAT CR110 and a shaper amplifier CREMAT CR200 (shaping time 8 microseconds).
See Fig. 2.

Fig. 2.6. 6-channel analogue boards.

2.5 *SAMADHA Bonner Sphere spectrometer calibration*

SAMADHA Bonner Sphere spectrometer was calibrated using a reference Am-Be field at the Politecnico di Milano, see "*Neutron spectrometry of a lightly encapsulated* ^{241}*Americium–beryllium neutron source using two different Bonner Sphere Spectrometers*", Nuclear Inst. and Methods in Physics Research, A 927 (2019) 371–374.

Figure 2.7 shows the experimental calibration setup with the shadow-cone technique. The spheres were placed on an irradiation bench at 190 cm from ground. The source-to-cone distance (SCD) was 10 cm. The source-to-detector (SDD) distance was varied between 110 and 140 cm to keep the shadowing ratio (SR) between 1 and 2 (ISO 8529-2), see Table 4.1.

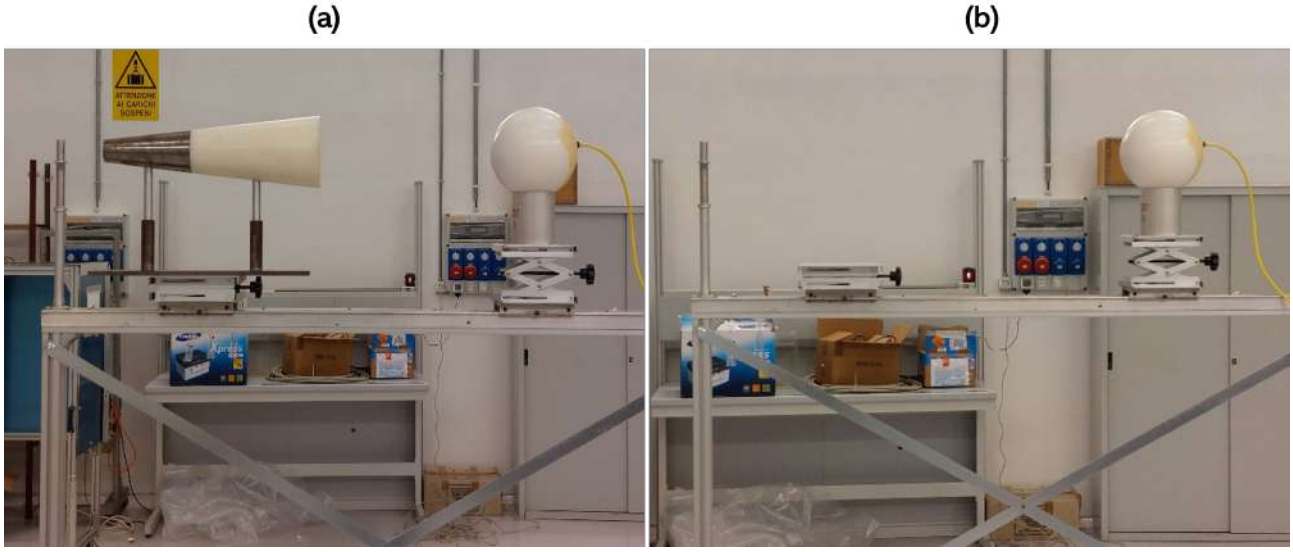

Figure 2.7. Experimental Calibration Setup (a) with and (b) without the shadow cone technique. The shadow cone technique evaluates the contribution of the scattered neutrons alone.

The acquired spectra can be seen in Figs. 2.8 and 2.9 in terms of dN/dE vs. E. The pulse height spectra for He-3 presents a full-peak corresponding to the whole Q-value of the absorption cross section (n, p) reaction. The ^{3}He(n,p)^{3}H reaction $Q = 0.764$ MeV, was used to calibrate the spectrometer in terms of Energy.

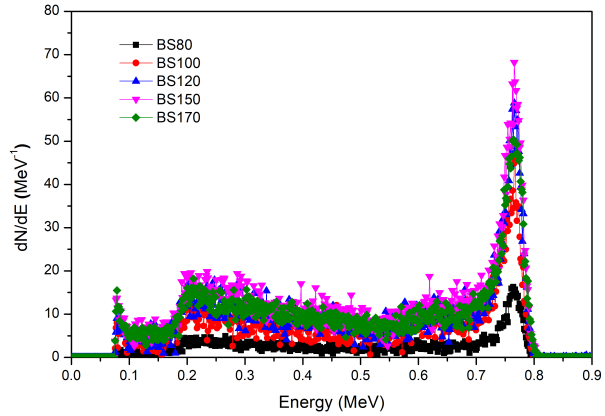

Figure 2.8. Spectrum of SAMADHA spheres

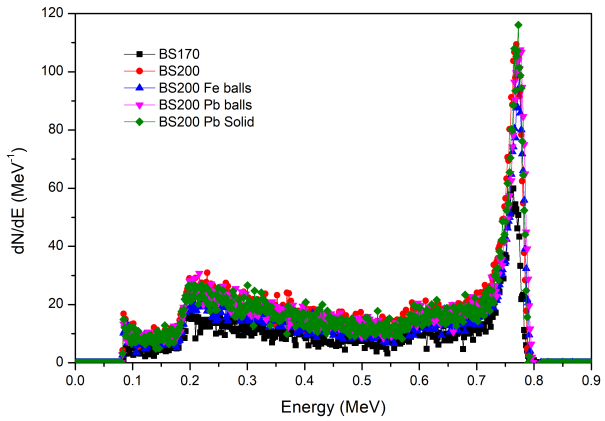

Figure 2.9. Spectrum of SAMADHA spheres.

The BSS response matrix, calculated with the Monte Carlo MCNP code, see Annex 1, was validated by comparison with the calibration experiment.

Table 2.2 compares the simulated BSS response of the unit fluence of ^{241}Am-Be to the experimental values. There is very good agreement in the calculated and simulated measurements.

Table 5. Counts obtained by folding the response functions and comparison with the June experimental measurements.

Sphere	**R $_{Calc}$**	**CPS**	**CPS / R $_{Calc}$**
80	0.18	1.99	11.2
100	0.40	4.47	11.2
120	0.63	7.25	11.5
150	0.89	10.34	11.6
170	1.03	12.23	11.9
200	1.12	13.03	11.6
200 Fe balls	0.89	10.43	11.7
200 Pb balls	1.04	12.39	12.0
		Overall SD	2.27%

The standard deviation of the experiment/simulation ratio, as small as 2%, is regarded as the overall uncertainty of the simulation model.

3. DOIN (CNTT) 2021

The DOIN project consits of prototyping a wearable electronic neutron personal dosimeter designed for the health protection of workers exposed to neutrons in the electronuclear, medical, civil engineering, oil & gas, mining and particle accelerator sectors.

The dosemeter is protected by patent 10/05/2021 - IT 102019000009741.

Two analog cards where the neutron detectors that will have to acquire the signals are inserted; The digital motherboard that interprets the signals coming from the two analog cards and passes them to the display card; The display board on which the results of the counts and their relationship in real time are displayed; The power supply board that redirects the power supply to the other boards and detectors (± 12 V to the analog ones, 3.3 V to the motherboard and to the display, 3.8 for the sensor bias). The entire system will be powered by a 1100 mAh at 3.8 V.
The mechanical parts were manufactured by the INFN-LNF SPCM. The dosimeter assembled with the cards can be seen in Fig. 3.1
The calibration of the device was performed at the Politecnico di Milano in the neutron metrology laboratory using a ^{241}Am-Be source. This measurement has shown that the dosimeter response does not change as a function of the angle, as required by the international dosimetry standards.

Fig. 3.1 Assembled dosemeter.

Calibrations were performed in neutron fields to verify the energy-independence of the response
- Thermal neutron fields: HOTNES source at ENEA in Frascati
- Epithermal neutron fields: EPINES source at ENEA in Frascati
- Fast neutron fields: source of ^{241}Am-B in the air

The dosemeter internally calculates an "energy index" q that can be related to the calibration factor, thus making the response highly energy independent. See Fig. 3.2.

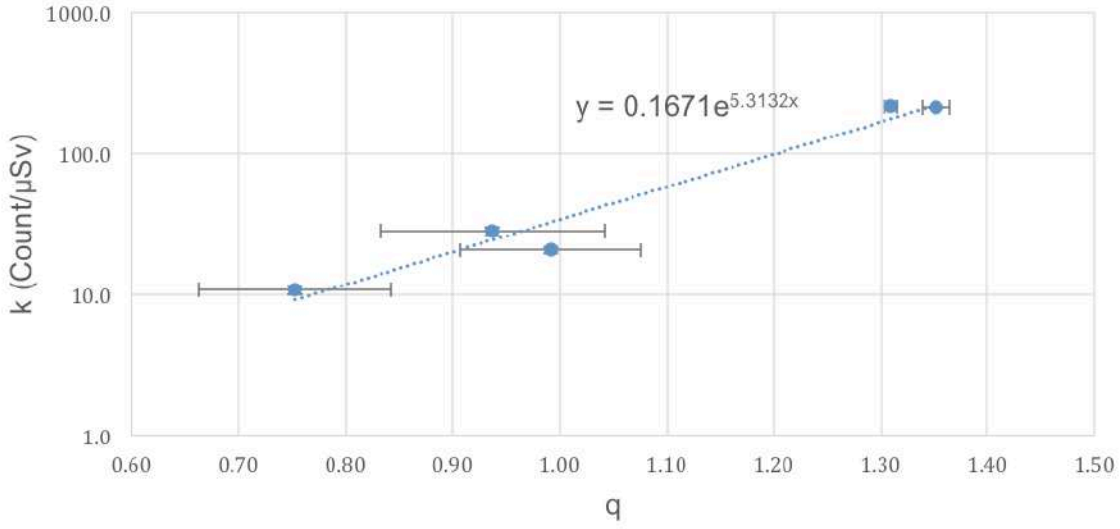

Fig. 3.2. Calibration factor as a function of the energy index, q.

Publications

[1] R. Bedogni, A. Sperduti, A. Pietropaolo, M. Pillon, A. Pola, J.M. Gomez-Ros. Nucl. Instrum. Methods Phys. Res. A 843 (2017) 18–21.

[2] R. Bedogni, A. Pietropaolo, J.M. Gomez-Ros, Appl. Radiat. Isot. 127 (2017) 68–72.

[3] A. Sperduti, M. Angelone, R. Bedogni, G. Claps, E. Diociaiuti, C. Domingo, R. Donghia, S. Giovannella, J.M. Gomez-Ros, L. Irazola-Rosales, S. Loreti, V. Monti, S. Miscetti, F. Murtas, G. Pagano, M. Pillon, R. Pilotti, A. Pola, M. Romero-Exposito, F. Sanchez-Doblado, O. Sans-Planell, A. Scherillo, E. Soldani, M. Treccani, A. Pietropaolo. J. Instrum. 12 (2018) P12029.

[4] Valeria Monti, Marco Costa, Elisabetta Durisi, Ettore Mafucci, Luca Menzio, Oriol Sans- Planell, Lorenzo Visca, Roberto Bedogni, Matteo Treccani, Andrea Pola, Davide Bortot, Katia Alikaniotis, Gianrossano Giannini, Jose Maria Gomez-Ros. The e_LiBANS facility: a new compact thermal neutron source based on a medical electron LINAC. Nuclear Inst. and Methods in Physics Research, A 953 (2020) 163154.

[5] V. Monti, E. Durisi, L. Menzio, O. Sans-Planell, M. Costa, L. Visca, M. Ferrero, R. Bedogni, M. Treccani, K. Alikaniotis, G. Giannini, The E_LiBANS project: thermal and epithermal neutron sources based on a medical Linac. Applied Radiation and Isotopes, accepted for publication (ARI_2019_902).

[6] R. Bedogni, A. Lega, A. Calamida, V. Monti, A. I. Castro-Campoy, L. Menzio, T. Napolitano, A. Pola, D. Bortot, A. Pietropaolo, M. Costa and S. Altieri. NCT-WES: A new single moderator directional neutron spectrometer for neutron capture therapy. Experimental validation. EPL, 134 (2021) 42001.

[7] Alevra, A.V., Thomas, D.J., 2003. Neutron spectrometry in moxed fields: multisphere spectrometers. Radiat. Prot. Dosim. 107 (1e3), 37e72.

[8] ISO, International Standardization Organization, Reference Neutron Radiations - Part 2: Calibration Fundamentals of Radiation Protection Devices Related to the Basic Quantities Characterizing the Radiation Field. ISO 8529-2 (2000)

[9] Bedogni, R.; Bortot, D.; Pola, A.; Introini, M. V.; Lorenzoli, M.; Gomez-Ros, J. M.; Sacco, D.; Esposito, A.; Gentile, A.; Buonomo, B.; Palomba, M.; Grossi, A. Experimental characterization of semiconductor-based thermal neutron detectors. NIM A 780 (2015) 51-54.

[10] R. Bedogni, A. Calamida, A.I. Castro-Campoy, J.M. Gomez-Ros, A. Lega, M. Moraleda, A. Pietropaolo, S. Altieri. Modelling the response of semiconductor based thermal neutron detectors with MCNP 6.2 and PHITS. Nuclear Inst. and Methods in Physics Research, A 1018 (2021) 165855.

[11] R. Bedogni, C. Domingo, A. Esposito, F. Fernandez. FRUIT: an operational tool for multisphere neutron spectrometry in workplaces. Nucl. Instr. Meth. A 580, 1301–1309 (2007).

[12] R. Bedogni, J.M. Gomez-Ros, M. Costa, V. Monti, E. Durisi, O. Sans Planell, L. Menzio, D. Flammini, F. Moro, M. Pillon, A. Pietropaolo. An active Bonner sphere spectrometer for intense neutron fields, Nuclear Instruments and Methods in Physics Research Section A: Accelerators, Spectrometers, Detectors and Associated Equipment, 940, 2019,Pages 302-306.

[13] Amgarou, K., Bedogni, R., Domingo, C., Esposito, A., Gentile, A., Carinci, G., Russo, S., Nucl. Instrum. Methods A 654 (2011) 399.